

Stop talking to me—a communication-avoiding ADER-DG realisation*

D.E. Charrier[†] T. Weinzierl[†]

January 29, 2018

Abstract

We present a communication- and data-sensitive formulation of ADER-DG for hyperbolic differential equation systems. Sensitive here has multiple flavours: First, the formulation reduces the persistent memory footprint. This reduces pressure on the memory subsystem. Second, the formulation realises the underlying predictor-corrector scheme with single-touch semantics, i.e. each degree of freedom is read on average only once per time step from the main memory. This reduces communication through the memory controllers. Third, the formulation breaks up the tight coupling of the explicit time stepping’s algorithmic steps to mesh traversals. This averages out data access peaks. Different operations and algorithmic steps are ran on different grid entities. Finally, the formulation hides distributed memory data transfer behind the computation aligned with the mesh traversal. This reduces pressure on the machine interconnects. All techniques applied by our formulation are elaborated by means of a rigorous task formalism. They break up ADER-DG’s tight causal coupling of compute steps and can be generalised to other predictor-corrector schemes.

1 Introduction

Hyperbolic equation systems in their first order formulation

$$\frac{\partial Q}{\partial t} + \nabla \cdot F(Q) + \sum_{i=1}^d B_i(Q) \frac{\partial Q}{\partial x_i} = S(Q) + \sum \delta \quad \text{with } Q : \mathbb{R}^{d+1} \mapsto \mathbb{R}^m \quad (1)$$

describe important wave phenomena from science and engineering. $d \in \{2, 3\}$ is the spatial dimension supplemented by time. For $m = 1$ equation (1) is scalar. In the ExaHyPE project [2] underlying this work, we focus on astrophysical and seismic phenomena: We want to obtain a better understanding of the long-range behaviour of earthquakes impacting critical infrastructure—this underlies seismic risk assessment—and we want to virtually search for gravitational waves emitted by rotating binary neutron stars or black holes. Advance in both fields hinges on better and faster numerical tools, such that we can increase the level of detail of the simulation, the time spans we study and the overall domain under examination. Solutions to (1) are often characterised by features spanning multitudes of scales in space that appear, move and disappear. Numerical observations hence have to cover large scales both in space and time, while an efficient numerical method to solve (1) has to be accurate, it requires a mesh that is dynamically adapted to localised features, and it requires an implementation delivering MFLOPS/s.

Explicit ADER-DG [8, 19] on adaptive Cartesian meshes derived from spacetrees [23, 22] promisingly candidates as tool as it yields very high spatial and temporal accuracy. It is a discontinuous Galerkin scheme and thus fits straightforwardly to nonconformal adaptive mesh refinement (AMR). In ADER-DG’s mindset, a weak formulation in space and time yields a

*The underlying project has received funding from the European Union’s Horizon 2020 research and innovation programme under grant agreement No 671698 (ExaHyPE). All software is freely available from www.exahype.eu.

prediction of how the solution would evolve within each cell if we were allowed to neglect the impact of neighbouring cells. This is called predictor step. The arising jumps along cell interfaces then are subject to a Riemann solver. In a final wrap-up, ADER-DG combines the predictor’s solution with the Riemann solve to obtain the solution at the subsequent time step. It is an explicit predictor-corrector scheme. The present paper studies for the first time ADER-DG’s data storage, data movement and data exchange characteristics in detail. We expect future machines to be equipped with enormous compute power. Transferring data from the memory into the chip and exchanging data between cores and nodes thus will become a severely limiting factor as these data movements require energy [6]. Our paper therefore uncovers both ADER-DG’s potential and fundamental challenges w.r.t. supercomputing. From hereon, it introduces techniques that make ADER-DG implementations single-touch, i.e. read each unknown only once per time step. It analyses whether and how the scheme becomes fit for exascale computing where it is key to reduce data movements.

For our applications, $\delta : \mathbb{R}^{d+1} \rightarrow \mathbb{R}^m$ in (1) models earthquake point sources while non-conservative operators $B_i(Q) : \mathbb{R}^{d+1} \rightarrow \mathbb{R}^{m \times m}$ anticipate material parameter changes. In astrophysics, we find the B_i modelling space-time curvature and the conservative flux $F(Q) : \mathbb{R}^{d+1} \rightarrow \mathbb{R}^{m \times d}$ modelling the relativistic evolution of magnetic material. Yet, the generality of the present paper allows us to transfer all insight to any other wave equation that can be phrased in the form of (1). The present discussion is not restricted to the two ExaHyPE application areas only. The rigour and generality of the proposed analysis and techniques furthermore imply that our insights can be transferred to many other predictor-corrector schemes; notably Finite Volumes which is a special case of our scheme. Finally, we detail and generalise the concept of communication-avoiding algorithms in the present manuscript and classify aspects of ADER-DG within this terminology.

The studied ADER-DG schemes rely on high order polynomials $p \in \{2, \dots, 9\}$ to span the solution in space and time. Despite the high-order, ADER-DG remains a one step scheme— one triad of prediction, Riemann solve and correction yields the next time step’s solution— where overall high order convergence is experimentally demonstrated [7, 10]. Once ADER-DG is combined with a Finite Volume (FV) limiter [8] it becomes robust despite the presence of shocks: the high order representation is temporarily and locally replaced with FV on a regular Cartesian patch. Particular characteristics of ADER-DG render it a particular promising candidate for high-performance computing. Yet, the very same characteristics pose realisation challenges w.r.t. current and future supercomputers [6]. First, ADER-DG’s high order polynomials spanning both space and time imply that each grid cell carries a significant number of degrees of freedom. Taking a cell from the main memory and writing its updates back to memory thus is bandwidth-demanding. Parts of these data are even required three times per time step though the Riemann solve and the correction typically have low arithmetic intensity. Second, ADER-DG’s single-step character involving only one Riemann solve per time step implies that solution and (normal) flux jump between the predicted cell solutions have to be exchanged only once per time step. Two strong synchronisation points per time step (the exchange of the Riemann input data plus the eigenvalues determining the CFL condition) plus the fact that each Riemann solve per se is computationally cheap however render the algorithmic blueprint latency- and load balancing-sensitive. Finally, modifications of the grid, the spatial discretisation paradigm and the possibility to choose a unique time step size per cell after each and every time step fit seamlessly into the discontinuous Galerkin paradigm. Conforming or balanced grids [18] and coordinated time step sizes on cells are not inherently required, while the fallback to FV injects robustness. Yet, this flexibility modifies the data flow pattern all the time, and it renders the cost per cell difficult to predict. The three properties face a machine generation where bandwidth is a scarce resource, rigorous synchronisation struggles to scale and runtime and latency are sensitive to communication pathways [6].

We propose to cast ADER-DG into a task language where each algorithmic step (predictor, Riemann, corrector) defines a set of tasks of one type. Temporal dependencies between the steps respective task types then are given by ADER-DG. Our grid instantiates the tasks plus their dependencies. It yields a partial order. While task-based formalisms are well-established, we are not aware of any similar formalism of our predictor-corrector scheme that clearly distinguishes task types, task dependencies, and task graph instantiation. A

distinction however is important: Our grid and, hence, our task graph may change in each time step. Since the partial order on the tasks does not impose a spatial order on the cells, since an assembly of any task graph is unnecessary if a mesh already encodes it, and since this task graph is subject to frequent changes and thus would be expensive to assemble and maintain, we make the grid traversal itself issue the tasks. We work task assembly-free. Our work shows that it is reasonable to shift all tasks along the simulation time axis; some even by half a grid sweep which makes the very first traversal trigger only half of the actions required to complete one time step. As long as the CFL constraints evolve smoothly, this allows us to rewrite ADER-DG optimistically with single-touch semantics [21]. Each cell’s data are only read/written once per time step. The approach furthermore allows us to hide all distributed memory data exchange behind the actual grid traversal and the other, expensive tasks. If time steps evolve non-smoothly or the limiter kicks in, the data access cost of our scheme double as we have to roll the solution partially back. Yet, they still remain better than for a straightforward predictor-corrector implementation which maps each algorithmic step onto one grid sweep.

The remainder is organised as follows: We first contextualise our work w.r.t. communication-avoiding algorithms (Sect. 2). Next, we revise ADER-DG briefly and clarify which mesh data structures we rely on (Sect. 3), before we state our main achievements (Sect. 4). In Sect. 5, we break down the algorithm’s steps into tasks and discuss techniques how to rearrange those tasks to make them communication-avoiding. We continue with an analysis of the arising realisation (Sect. 6) which predicts to which degree our techniques make the algorithm’s implementation bandwidth- and memory bus-modest and thus fit to our notion of communication-avoiding. We continue with experimental results before we close the discussion in Sect. 8.

2 Communication-avoiding algorithms

Our contribution is the rewrite of ADER-DG in terms of a communication-avoiding algorithm expressed in a task language. Our notion of communication-avoiding generalises the classic term ([5] and references therein) as it comprises

1. the elimination of data transfer volume [3, 5]. While we elaborate appropriate techniques in [9, 21] and clarify in the present manuscript how they integrate seamlessly into our realisation, the major contribution here is to reduce ADER-DG’s memory footprint from a space-time footprint into a d -dimensional footprint.
2. the elimination of the data transfer frequency. We fuse two data exchange steps into one data exchange and restrict ourselves to single-touch algorithms where each data item is read and written only once [17, 21]. Only in few cases, our approach requires redundant computations.
3. the homogenisation of data transfer. We ensure that the demand for data does not fluctuate significantly over the compute time. Notably, communication bursts are avoided. This ensures that data transfer facilities are not idle over long time spans and reduces time intervals when they are oversubscribed.
4. the overlapping of data transfer with communication [5, 11, 13]. This avoids that the code bumps into waits as incoming data are, in the best case, already available when they are needed. This property results from a reordering of algorithmic steps such that different arithmetic operations are localised and thus, once completed, all affected data can travel through interconnects until the next grid sweep hits a mesh cell again.
5. the localisation of data transfer [13]. Explicit time stepping natively exchanges data only between neighbouring cells and thus tickboxes this rubric. Yet, our contribution also covers temporal data access proximity, i.e. shared memory data transfer and cache effects [14]. Activities following each other work on spatially near data and data is not temporarily filed in main memory.

We consider all communication-avoiding techniques not only to affect distributed memory but also to apply to memory access and multicore communication. While we derive our communication-avoiding techniques for ADER-DG and FV, the ideas should apply to many predictor-corrector schemes. The above classification is generic.

3 ADER-DG on spacetime meshes

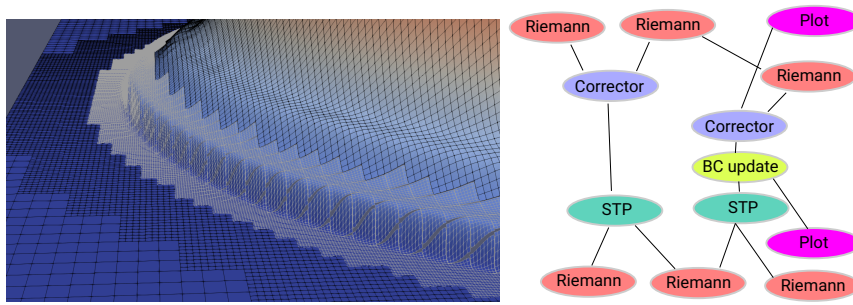


Figure 1: Left: Adaptive Cartesian grid of a $2d$ simulation where the solution is extruded in the third dimension. Right: Characteristic ADER-DG task graph.

Our grids arise from a standard spacetime construction scheme based upon tripartitioning [23]. We embed the computational domain into a square or cube, respectively, and cut this cube equidistantly into three parts. This yields nine or 27, i.e. 3^d , new hypercubes with d being the spatial dimension. We decide per hypercube whether to continue recursively, and thus end up with an adaptive Cartesian grid (Fig. 1) consisting of a set \mathbb{T} of squares or cubes, respectively. We call them *cells*.

Each cell $c \in \mathbb{T}$ within the adaptive Cartesian grid holds a part of the ADER-Discontinuous Galerkin (DG) solution $Q_h(T)$. We store $m \cdot (p+1)^d$ coefficients per DG cell. They are used to cellwisely span a p th order polynomial modelling all m solution components from (1). The polynomials are expressed via a tensor-product Lagrange basis with Gauss-Legendre collocation points. The support of the basis functions is limited to the interior of c . Values of polynomials along cell faces, i.e. extrapolated from one cell side or the other, usually differ—which renders the global solution discontinuous in space.

The following recapitulation of ADER-DG’s algorithmic steps neglects sources and non-conservative terms for simplicity. We start from a weak formulation of (1) and discretise it in space. Let our weak formulation be a Ritz-Galerkin formulation, i.e. let the test and shape space hold the same functions multiplied by p th order time-dependent polynomials. Partial integration over the time interval $(T, T + \Delta T)$ and integration over the cells c by applying Green’s theorem then yield an implicit formula for the update $D_h = Q_h(T + \Delta T) - Q_h(T)$. ADER-DG’s fundamental idea is to replace Q_h and, thus, $F(Q_h)$ with an “estimated” evolution Q_h^* within $(T, T + \Delta T)$ plus an additional term. Q_h^* is a predicted solution in space and time—the *space-time predictor*—that results from a set of implicit solves of (1) restricted to individual cells. We obtain the discrete variational problem [8]

$$\int_c v_h D_h dx = \int_T^{T+\Delta T} \int_c \nabla v_h : F(Q_h^*) dx dt - \int_T^{T+\Delta T} \oint_{\partial c} v_h [F(Q_h^*) \cdot n]_{\partial c} ds dt. \quad (2)$$

Three algorithmic steps that decompose into further tasks numerically invert (2).

ADER-DG step 1: compute space-time predictor To obtain a prediction Q_h^* , we study the individual cells c independent of each other, i.e. we neglect that the solutions of neighbouring cells interfere. This gives

$$\text{STP:} \quad \forall c \in \mathbb{T}: \quad \int_T^{T+\Delta T} \int_c \left(\frac{\partial Q_h^*}{\partial t} + \nabla \cdot F(Q_h^*) \right) \varphi_h dxdt = 0. \quad (3)$$

Cell-wisely, it is an implicit scheme that we solve through Picard iterations. Lagrange polynomials with Gauss-Legendre collocation points plus Green’s theorem yield a quadrature-free formulation with sparse operators. Yet, the number of required Picard iterations per cell is not known and the solve (of one step) of (3) remains arithmetically expensive.

STP works with the PDE solution in space and time, i.e. a $d + 1$ -dimensional dataset. Technically, it decomposes into a task `predict` that spans the polynomial in space and time, and a task `extrapolate` that yields the predicted solution plus its flux along the normal on the cell faces. The extrapolation is needed by the next step.

ADER-DG step 2: solve Riemann problem The projection of both the solution Q_h^* and its normal flux $F(Q_h^*) \cdot n$ of (3) onto the cell faces exhibits jumps. n is the generic normal vector spanning a row-wise scalar product. $Q_h^{*\pm}$ and $F(Q_h^*)^\pm \cdot n$ from one side (+) and the other (−) typically differ; not only by a sign. ADER-DG’s second step thus replaces the discontinuous expression by a numerical flux. It applies a Rusanov solver. This yields

$$\text{Riemann:} \quad \forall c \in \mathbb{T}: \quad [F(Q_h^*) \cdot n]_{\partial c} = F_h^* \text{ with } F_h^* = F_h^*(Q_h^{*\pm}, F(Q_h^*)^\pm n). \quad (4)$$

The left and right predicted solution onto a face are required as input, as well as the left and right predicted solution flux along the normal. `Riemann` yields flux contributions over $(T, T + \Delta T)$ along the cell faces. We formalise it as a task `solveRiemann` determining F_h^* , which is formally a $F_h^*(t)$ with $t \in (T, T + \Delta T)$. We note that holding $F_h^{*\pm}$ is redundant for $B = 0$ as the two sides differ only by their sign. Yet, it allows each cell to work with “its” Riemann solve result and applies without modifications to $B \neq 0$.

ADER-DG step 3: correct predicted solution We finally return to the non-local formulation (2) which is made globally explicit through Q_h^* and $F_h^{*\pm}$. This explicit forward operator evaluation renders ADER-DG a single-step scheme and decomposes (2) into a cell-local contribution which we have available from ADER-DG’s first step plus a contribution from the Riemann problem. We add the Riemann solve’s result to the predicted value. It is corrected. Hence, our third step is denoted as `Corrector`.

The `Corrector` step decomposes into a task `integrateVolume` collapsing the space-time polynomial of the predictor onto $T + \Delta T$, an `integrateFace` task integrating over the result of the Riemann solve and thus projecting the space-time evolution along the cell faces onto the cells’ spatial data at $T + \Delta T$, an `update` task which swaps D_h into the location of Q_h , and `calculateTimeStep` which returns an admissible time step size ΔT_{adm} for the next time step due to the CFL condition. The overall predictor-corrector sequence equals

$$Q_h(T + \Delta T) = (id + \text{integrateVolume} \circ \text{predict} + \text{integrateFace} \circ \text{solveRiemann} \circ \text{extrapolate} \circ \text{predict}) Q_h(T) \quad (5)$$

$$= (id + (\text{integrateVolume} + \text{integrateFace} \circ \text{solveRiemann} \circ \text{extrapolate}) \circ \text{predict}) Q_h(T) \quad (6)$$

as operator evaluation with its memory footprints displayed in Table 1.

Time stepping If the combination of PDE plus initial and boundary conditions yields a sufficiently smooth solution, the convergence of ADER-DG is numerically verified to converge with optimal order; as long as ΔT does not harm the CFL condition [7, 10]. Two requirements arise for our implementation from this statement: On the one hand, a robust implementation has to determine ΔT_{adm} numerically, and it has to ensure these are not exceeded. On the other hand, a p th order scheme is known to yield oscillating solutions and non-physical values (such as negative densities) once discontinuous solutions (“shocks”) arise [12]. A robust time stepping thus has to be able to identify localised nonphysical solutions (*troubled cells*) after

Table 1: Memory requirements per task as number of double values (degrees of freedom): how much data per task is read in and how much data is written. All data is normalised per task and per cell c or neighbour cell pair c_a, c_b . We group the tasks along three steps **STP**, **Riemann** and **Corrector**.

Task	in	out	Remarks
STP			
<code>predict(c)</code>	$m \cdot (p+1)^d$	$(d+1) \cdot m \cdot (p+1)^{d+1}$	determine Q_h^* and $F(Q_h^*)$
<code>extrapolate(c)</code>	$(d+1) \cdot m \cdot (p+1)^{d+1}$	$4d \cdot m \cdot (p+1)^d$	extrapolate Q_h^* and $F(Q_h^*) \cdot n$ to all $2d$ faces of a cell
Riemann			
<code>solveRiemann(c_a, c_b)</code>	$4d \cdot m \cdot (p+1)^d$	$2d \cdot m \cdot (p+1)^d$	may store result in one of the input arrays
Corrector			
<code>integrateVolume(c)</code>	$d \cdot m \cdot (p+1)^{d+1}$	$m \cdot (p+1)^d$	integrate predicted $F(Q_h^*)$
<code>integrateFace(c)</code>	$2d \cdot m \cdot (p+1)^d$	$m \cdot (p+1)^d$	accumulate in output data structure of <code>integrateVolume</code>
<code>update(c)</code>	$m \cdot (p+1)^d$	$m \cdot (p+1)^d$	add D_h to Q_h
<code>calcTimeStep(c)</code>	$m \cdot (p+1)^d$	1	

the **Corrector**, roll back to the old time step and recompute the solution through Finite Volumes. The Finite Volumes act as limiter.

Global time stepping has to restrict ΔT_{adm} once all **Corrector** tasks have terminated, before it broadcasts the next time step size to use to all ranks. Local time stepping, i.e. time stepping where the time step size depends with $\Delta T_{adm}/3^\ell$ on the mesh size (ℓ is the spacetime level) equals global time stepping w.r.t. the exchange of ΔT_{adm} . Yet, the restriction can be temporarily sparsified, i.e. is to be done for the coarsest cells only. Local time stepping in ADER-DG advances cells on the levels ℓ and $\ell+1$ through **STP**. As ΔT depends on ℓ , the finer cells on level $\ell+1$ now can evaluate “their” **Riemann** problem and **Corrector** step. This Riemann solve tackles the jump adjacent to the coarser cell partially in time. It thus yields a partial update of the coarse neighbour’s next time step’s solution through `integrateFace`. Since we rely on tripartitioning, the coarser cells on level ℓ cannot run the Riemann solve until the adjacent finer cells on level $\ell+1$ have made three time steps. This pattern extends to non-balanced grids recursively, yet assumes that ΔT depends smoothly on the mesh size. If this does not hold, more than three steps per finer grid level are required. Global ΔT coordination in this case becomes necessary. As a result, we restrict our analysis to global time stepping. Local time stepping realises global data flow and data exchange along the same lines though with fewer reductions.

Finite Volume limiter Following [8, 25], we augment the ADER-DG scheme with adaptive mesh refinement plus subcell limiting. Let *troubled* cells be cells where the hosted ADER-DG solution is inadmissible. It oscillates or does physically not make any sense for example. Besides the ADER-DG data, we make these cells host an additional regular Cartesian subgrid of the resolution $(2p+1)^d$ and advance a Finite Volumes (FV) scheme on this subgrid forward in time. After each time step, averaging projects the FV solution back onto the DG space and then assesses whether the FV solution can be represented by the polynomials without harming the admissibility. Once this is the case for all m components, we remove the Cartesian FV grid, remove the troubled marker and continue with the ADER-DG scheme within the cell.

Corollary 1 *Finite Volume schemes with Rusanov fluxes or a MUSCL-Hancock Riemann solver neglecting cell interactions that are not face-connected can be cast into our predictor-corrector formalism.*

The proofs (Appendix A) are technical but clarify that it is sufficient to study plain ADER-DG’s memory movement and communication-behaviour only. If we couple ADER-DG with FV, both solvers exhibit the same communication pattern. All communication characteristics change only quantitatively.

4 Statements on ADER-DG

Let the term *element-wisely* characterise a grid-based algorithm where an operator on a cell has no access to any other cell. It may solely access a cell’s data and its faces. Element-wise operators working on faces may access only face data. Let the term *single-touch* characterise an implementation which reads and writes unknowns only once per time step [21].

Constraint 1 *Multiple STP evaluations have to be avoided.*

We anticipate the experimental insight that the prediction in variation (6) dominates the computational cost. Though (5) and (6) are symbolically the same, only (6) thus is computationally feasible.

Constraint 2 *We focus on problems where (i) one solution snapshot Q_h does not fit into the registers and machine caches, and (ii) one cell’s space-time polynomial, i.e. all data read and written by **predict**, fit into the registers/caches.*

Any more relaxed assumption on problem sizes or machine configurations relaxes our single-touch statements. We abstract from different cache levels and their multifaceted impact on real-world performance. For most machines, our memory transfer statements apply at least to the last-level cache.

Theorem 1 (Memory footprint theorem) *Even though ADER-DG’s prediction spans a space-time polynomial, it is sufficient for an element-wise ADER-DG realisation to store a space-time hull of each space-time hypercube in the mesh persistently. This hull has to encode flux contributions along faces besides solution data.*

Theorem 2 (Weak element-wise single-touch theorem) *There is a $1 \leq C_{\text{rerun}} < 2$ such that the predictor-corrector operator in the formulation (6) can be realised element-wisely with C_{rerun} data reads per time step.*

Both proofs are constructive and apply the techniques from Sec. 5. An experimental $C_{\text{rerun}} \approx 1$ renders the single-touch property strong. If we skipped the term element-wisely, the theorem would become trivial as (6) would be just one global explicit operator consisting of two components.

Corollary 2 *A direct element-wise realisation of (6) can not be single-touch.*

This proof is technical (Appendix B) and relies on the fact that the steps are subject to a partial temporal order (Fig. 1)

$$\forall c_a, c_b \in \mathbb{T} : \text{STP}(c_a) \sqsubseteq_{\text{before}} \text{Riemann}(c_a, c_b) \quad \wedge \quad \text{Riemann}(c_a, c_b) \sqsubseteq_{\text{before}} \text{Corrector}(c_a). \quad (7)$$

While it motivates some of the techniques we use later to construct a single-touch element-wise algorithm, it demonstrates that applying an isolated, single technique alone is not sufficient.

5 Communication-avoiding, task-based ADER-DG

ADER-DG tasks are subject to the temporal constraints (7). Additional tasks may enter the task graph:

1. If requested by the user, we insert a `Plot` task after the `Corrector`.
2. A time step size computation follows the solution update.
3. If inadmissible high order solutions are to be expected, we merge an `Admissible` task into `Corrector` which can label cells as *troubled*. If a cell becomes troubled, we roll back to the previous solution, insert the FV’s patch representation of this solution, and add an additional STP task rerunning the time step with FV.

4. If a cell is subject to FV, we add an additional **Reconstruct** step after the corrector that projects the Finite Volume solution back onto the higher-order ADER-DG representation. If a FV solution could validly be represented by the polynomial, the cell’s state is reset and the Cartesian patch data are erased.
5. To couple ADER-DG solutions with FV, there is a helper task type inserting “non-troubled” FV cells around the troubled ones. Such a halo solely represents the DG solution as Finite Volumes, yet does not run FV updates. The cells allow the FV scheme to compute fluxes on the patch faces of troubled cells. They act as coupling layer between ADER-DG and the limiter.
6. If adaptive mesh refinement (AMR) is used, additional AMR tasks realising the refinement and coarsening criteria are to be inserted.
7. Additional tasks for boundary and initial conditions—both overwrite the computed solution with a prescribed or altered data—complete the picture.

Algorithm 1 One time step of the simplest version of ADER-DG without limiter as traditional, sequential pseudo code. Left: Standard time stepping. Right: Shifted time stepping. $C_{\Delta T} \leq 1$ is a chosen security factor.

<pre> 1: while $T < T_{final}$ do 2: for $c \in \mathbb{T}$ do 3: predict(c) 4: extrapolate(c) 5: end for 6: for face-connected $c_a, c_b \in \mathbb{T}$ do 7: solveRiemann(c_a, c_b) 8: end for 9: $\Delta T_{adm} \leftarrow \infty$ 10: for $c \in \mathbb{T}$ do 11: integrateVolume(c) 12: for all faces f of c do 13: integrateFace(f) 14: end for 15: update(c, f_1, f_2, \dots) 16: $\Delta T_{adm} \leftarrow \min\{\Delta T_{adm}, \text{calcTimeStep}(c)\}$ 17: end for 18: $T \leftarrow T + \Delta T$ 19: $\Delta T \leftarrow C_{\Delta T} \cdot \Delta T_{adm}$ 20: end while </pre>	<pre> 1: while $T < T_{final}$ do 2: for face-connected $c_a, c_b \in \mathbb{T}$ do 3: solveRiemann(c_a, c_b) 4: end for 5: $\Delta T_{adm} \leftarrow \infty$ 6: for $c \in \mathbb{T}$ do 7: integrateVolume(c) 8: for all faces f of c do 9: integrateFace(f) 10: end for 11: update(c, f_1, f_2, \dots) 12: $\Delta T_{adm} \leftarrow \min\{\Delta T_{adm}, \text{calcTimeStep}(c)\}$ 13: end for 14: $T \leftarrow T + \Delta T$ 15: $\Delta T \leftarrow C_{\Delta T} \cdot \Delta T_{adm}$ 16: for $c \in \mathbb{T}$ do 17: predict(c) 18: extrapolate(c) 19: end for 20: end while </pre>
--	--

Our ADER-DG scheme is defined over a computational grid. Given the grid plus the task dependencies stemming from (7), we obtain a global task graph per time step. We interpret the grid instantiating the task graph at hands of (7) [22]. As ADER-DG’s task dependencies are localised, we can run over the grid (in parallel) and issue the tasks directly per cell. There is no need to assemble the task graph.

If we translate ADER-DG’s steps straightforwardly into a traversal code, we obtain a sequence of loops (Alg. 1). The loop body per cell or face, respectively, is the actual task invocation. We refer to such an implementation as straightforward. One loop issuing STP with high arithmetic intensity is followed by two loops triggering computationally cheap tasks. Yet, we observe that, on the one hand, ADER-DG imposes only a partial order, and we observe that not all tasks have to be tied to “their” step. We can reorder and rearrange the execution order as long as all data remains consistent. On the other hand, ADER-DG does not enforce us to run the same operation on all grid entities. It allows us to run the predictor in one grid area, while another area performs Riemann solves. There is no need to align each grid

traversal with exactly one task type. These observations give rise to the following techniques. Throughout their presentation, we make a *realisation time step* comprise all three task types `STP`, `Riemann` and `Corrector`.

Technique 1 *Move tasks from one logical step into an earlier step such that they are ran as early as possible.*

This technique is data-centric as it helps to avoid capacity and conflict cache misses as well as register spilling.

Implication 1 *We evaluate `integrateVolume` directly after `predict` and evaluate `integrateFace` directly once `solveRiemann` has terminated. This allows us to eliminate temporary variables.*

`predict` spans the space-time polynomial. Applying the technique, this outcome is to be held only temporarily: It is passed over to `extrapolate` before we integrate it and discard the data. The integration is a task logically assigned to the `Corrector` step, i.e. we bring it forward. Its result is stored in D_h instead of the old time step’s Q_h as we have to preserve Q_h to facilitate rollbacks required for a FV intervention.

The technique is applied analogously to `integrateFace`. `solveRiemann` handles jumps over a face in space-time. `integrateFace` maps this data of spatial cardinality $m(p+1)^{d-1}$ plus a temporal dimension onto a contribution to the solution update D_h . Different to the space-time predictor, moving the integration from the `Corrector` into `Riemann` does not allow us to reduce the memory footprint. Adaptive time stepping requires us to hold $Q_h^{*\pm}$ and $F(Q_h^{*\pm}) \cdot n$ over the whole space-time span of a cell to determine (partial) $F_h^{*\pm} \cdot n$. Passing the two $F_h^{*\pm} \cdot n$ ingredients directly into `integrateFace` would violate our definition of cell-wisely.

Technique 2 *Run different tasks on different grid entities concurrently.*

Graph-based tasking systems model tasks as nodes in a graph and the task dependencies as edges. At one particular time, a tasking system may launch any task which has no pending dependencies anymore. Once a task terminates, the node plus all outgoing edges (data writes) are removed from the graph. The power of tasking [16, 24] results from the fact that different task types might be launched simultaneously.

This idea translates to grid-based solvers: When we run through the grid, we impose a spatial order on grid entities. We may launch the `Riemann` solve whenever we run into a face for the first time, i.e. when we read it from the main memory the first time (touch-first semantics). If we stick to a pure cell-wise traversal, the time when a face is “touched” for the very first time results directly from the cell ordering: if we enter a cell, we touch all of its faces; maybe some of them for the first time.

Implication 2 *When we enter a cell to perform `Corrector`, we analyse all of its 2d adjacent faces whether they have been read from main memory before. For faces that have not yet been used, we run the `Riemann` solve. As the `Corrector` issues the tasks from the `Riemann` step on-demand, `Corrector` and `Riemann` evaluations are intermixed throughout one grid sweep. We eliminate an explicit `Riemann` sweep.*

This technique is particularly interesting in the context of cache-oblivious algorithms [14]. Let a grid traversal minimise the time between when one cell is handled to the handling of any neighbour cell. The first cell’s `Corrector` requires the outcome of the `Riemann` solves of its faces. If not computed yet, it determines them. The neighbouring cell uses these face data, too. If the time in-between the two task executions is small, we have temporarily localised data access: the probability that the data still resides in cache is high. Traditional techniques to obtain such traversal orderings are loop blocking and space-filling curves [1]. In our experiments, we rely on the latter [23].

Technique 3 *Shift the tasks by half a grid sweep.*

We kick off the computation with an evaluation of `Riemann` and `Corrector`, before we run the first complete triad `STP,Riemann,Corrector`. Furthermore, we distinguish time step sizes ΔT_{adm} , ΔT_{old} and ΔT_{new} . `Riemann` and `Corrector` use ΔT_{old} . `STP` uses ΔT_{new} . After `STP`, we roll over $\Delta T_{old} \leftarrow \Delta T_{new}$. Formally, we recast the time stepping in (6) into a sequence of

$$\begin{aligned} \begin{pmatrix} Q_h \\ D_h \\ (Q_h^{*\pm}, F(Q_h^*)^\pm \cdot n) \end{pmatrix} (T + \Delta T) &= \begin{pmatrix} 1 & 0 & 0 \\ \text{integrateVolume} \circ \text{predict} & 0 & 0 \\ \text{extrapolate} \circ \text{predict} & 0 & 0 \end{pmatrix} \cdot \\ &\quad \underbrace{\hspace{10em}}_{\text{run STP of next time step already}} \\ \begin{pmatrix} 0 & 1 & \text{integrateFace} \circ \text{solveRiemann} \\ 0 & 0 & 0 \\ 0 & 0 & 0 \end{pmatrix} &\quad \begin{pmatrix} Q_h \\ D_h \\ (Q_h^{*\pm}, F(Q_h^*)^\pm \cdot n) \end{pmatrix} (T) \quad (8) \\ &\quad \underbrace{\hspace{10em}}_{\text{complete Corrector and Riemann started in previous sweep}} \end{aligned}$$

applications (Alg. 1). Here, `integrateVolume` is already merged into `STP` (cmp. Technique 1). While the operator matrices enlist `predict` twice, it has to be evaluated only once with the result temporarily held and passed into two follow-up tasks. As $\Delta T_{old} = 0$ throughout the first grid sweep, the very first composition of `Riemann` and `Corrector` does not modify the solution as the integrals in (3) and (4) degenerate.

Implication 3 *Let 3N grid sweeps through the grid be used by a straightforward ADER-DG realisation. Each sweep implements one ADER-DG step (predictor, Riemann, corrector). The Techniques 2 and 3 make the solve require $N + 1$ sweeps in total.*

Formalism (8) logically shifts the evaluation of ADER-DG by half a grid sweep: Half of the work of a subsequent time step is already done once a sweep terminates. We thus refer to this realisation variant as *shifted evaluation*. The approach resembles pipelining [11, 17]. Different to most pipelining, our shifts do however not introduce additional helper variables. D_h and $(Q_h^{*\pm}, F(Q_h^*)^\pm \cdot n)$ have to be held in memory anyway to facilitate roll backs for the limiter and local time stepping.

Implication 4 *Let $\Delta T_{adm} > T_{new}$. Technique 3 in combination with Technique 2 allows to realise, amortised, one realisation time step per grid sweep.*

The implication yields $1 \leq C_{\text{rerun}}$ in Theorem 2.

Technique 4 *Fuse tasks.*

Our shifted grid sweeps run through the cells of \mathbb{T} . Per cell, they analyse the $2d$ faces and trigger `Riemann` if the neighbouring cell connected through the face has not been traversed before. As soon as this cell preamble has terminated, the grid sweep triggers `Correction` and immediately afterwards `STP`. All orders obey (7). Algorithmically, this approach is similar to loop fusion. Some faces might still “wait” for a Riemann solve, while others already have finished their correction and projected Q_h^* and $F(Q_h^*)$ onto the faces again. From a cell’s point of view, we invert and fuse the task execution order: Per cell, `STP` is immediately launched after `Corrector`. This is made possible as we distinguish ΔT_{new} and ΔT_{old} . We fuse `Corrector` and `STP` (in this order). Also the concatenation of `integrateVolume` with `predict` is logically task fusion.

Implication 5 *Techniques 2, 3 and 4 read, amortised, each cell’s solution data Q only once per time step as long as $\Delta T_{adm} > T_{new}$.*

Even if a code does not physically fuse tasks, any output data of the first task remains in the cache as input to the second—subject to a sufficiently big cache—as we run the respective tasks directly after each other. Since we schedule our tasks ourselves through the grid traversal, no task stealing or thread switching can interfere.

Technique 5 *Be optimistic.*

The explicit nature of ADER-DG requires us to exchange ΔT_{adm} once a time step completes. This introduces two synchronisation points in our shifted implementation: the grid sweep itself plus the time step size synchronisation. Two optimistic modifications allow us to eliminate one synchronisation without loosing adaptive time step size choices. On the one hand, we run STP with ΔT_{new} ignorant of ΔT_{adm} : As soon as a corrector finishes, its cell is subject to the next predictor though other correction steps running concurrently or later still might reduce ΔT_{new} . On the other hand, we check if $\Delta T_{adm} < \Delta T_{new}$ after all STPs of one time step have terminated. If we find that our chosen time step size harms the CFL condition, we reset $\Delta T_{old} \leftarrow C_{\Delta T} \cdot \Delta T_{adm}$ and rerun the prediction.

A naive implementation would break out of the cell loop immediately once the CFL condition is harmed. We however note that this can be disadvantageous as we might run into rippling loop restarts. Running all STPs always, thus finishing all updates and ΔT_{adm} computations, and reducing ΔT_{adm} afterwards implies that the set of STPs is relaunched either not at all or exactly once. This is *optimistic time stepping* as all **Corrector**-STP task pairs are ran even though we might already know after the first few that the outcome of the second task pair is invalidated.

Implication 6 *Even if the optimistic assumption fails, our code requires at most two grid sweeps per realisation time step. As we may assume that not every time step harms the CFL condition, we obtain a real upper bound $C_{\text{rerun}} < 2$.*

In our implementation, we make $\Delta T_{new} = \frac{1}{2} (T_{old} + C_{\Delta T} \cdot \Delta T_{adm})$. As long as time step sizes are chosen too pessimistic, we make ΔT_{new} creep towards ΔT_{adm} .

6 Properties

With our four communication-avoiding techniques defined, we end up with a cell-wise algorithm (Alg. 2). Several properties arise directly.

Corollary 3 *The persistent memory footprint of our algorithmic realisation variant is*

$$\frac{2 + 6d}{(d + 1)(p + 1) + 1 + 6d} \leq 0.875$$

of the footprint of a straightforward element-wise ADER-DG implementation holding the output of the three ADER-DG steps explicitly.

Proof 1 *A three-step, straightforward element-wise ADER-DG implementation starts from Q_h to span the space-time polynomial. An STP epilogue derives explicitly the extrapolated predicted solution plus its flux contribution along the faces. The Riemann solver determines numerical fluxes which are stored on the face over the whole time span of the adjacent cells. For local time stepping, the adjacent cell with the smaller span determines “whole time span”.*

Technique 1 implies that we hold the space-time representation only temporarily as the outcome of `integrateVolume` is backed up in D_h . Also `integrateFace` directly accumulates all outputs into this array. D_h has to be held separately from Q_h as we have to give ADER-DG the opportunity to declare a time step as troubled and to fall back to FV. As `integrateVolume` and `integrateFace` are brought forward in simulation time, it is not possible to merge admissibility checks into the D_h update, i.e. D_h cannot be eliminated.

We combine these insights with the analysis from Table 1.

It is the predictor’s full space-time representation that we do not have to hold. We hold solely the space-time hull of each cell with additional flux data on the space-time faces. The memory pressure compared to a straightforward version reduces as the memory volume is shrunk. Our approach falls into the first rubric of communication-avoiding techniques.

Corollary 4 *Let $T_{3 \text{ steps}}$ be the time required to run the triad of STP, Riemann and Corrector as three separate grid sweeps. Let $T_{\text{STP}} < T_{3 \text{ steps}}$ be the time that is spent on a sole STP*

Algorithm 2 Our cell-based, shifted ADER-DG implementation relying on all introduced optimisation techniques.

```

1: while  $T \leq T_{final}$  do
2:   if  $\Delta T_{adm} < \Delta T_{new}$  then                                     ▷ Optimistic guess had been wrong
3:      $(\Delta T_{old}, \Delta T_{new}) \leftarrow C_{\Delta T} \cdot \Delta T_{adm}$                                        ▷ Reset time step sizes
4:     for  $c \in \mathbb{T}$  do                                             ▷ STP rerun is additional loop over cells
5:       predict( $c$ )
6:       extrapolate( $c$ )
7:       integrateVolume( $c$ )
8:     end for
9:   end if
10:   $\Delta T_{old} \leftarrow \Delta T_{new}$ 
11:   $\Delta T_{new} \leftarrow C_{\Delta T} \cdot \Delta T_{adm}$  or  $\Delta T_{new} \leftarrow 0.5(\Delta T_{old} + C_{\Delta T} \cdot \Delta T_{adm})$ 
12:  TIMESTEP( $\Delta T_{old}, \Delta T_{new}$ )                                     ▷ Either strict time step set or creeping average
13: end while
14: function TIMESTEP( $\Delta T_{old}, \Delta T_{new}$ )
15:   $\Delta T_{adm} \leftarrow \infty$ 
16:  for  $c \in \mathbb{T}$  do                                             ▷ Element-wise traversal
17:    for  $f \in$  adjacent faces of  $c$  do                               ▷ Riemann
18:      if  $f$  touched first time then
19:        solveRiemann( $f^+, f^-$ )
20:      end if
21:    end for
22:    for  $f \in$  adjacent faces of  $c$  do                               ▷ Corrector using  $\Delta T_{old}$ 
23:      integrateFace( $f$ )
24:    end for
25:    update( $c, f_1, f_2, \dots$ )                                       ▷  $f_1, f_2, \dots$  are adjacent faces of  $c$ 
26:     $\Delta T_{adm} \leftarrow \min\{\Delta T_{adm}, \text{calcTimeStep}(c)\}$ 
27:    predict( $c$ )                                                     ▷ Immediately kick off next STP
28:    extrapolate( $c$ )                                               ▷ subject to  $\Delta T_{new}$ 
29:    integrateVolume( $c$ )                                           ▷ anticipate Corrector task, hold only space-time hull
30:  end for
31: end function

```

sweep. T_{fused} is the time required to run one fused time step without any reruns. Let the used $\Delta T = C_{\Delta T} \cdot \Delta T_{\text{adm}}$ be damped by $C_{\Delta T} \leq 1$. Our communication-avoiding fused algorithm yields better time-to-solution than a straightforward approach if

$$1 \leq C_{\text{rerun}} < 1 + \frac{T_{3 \text{ steps}} \cdot C_{\Delta T} - T_{\text{fused}}}{T_{\text{STP}}}.$$

Proof 2 Our weak single-touch Theorem 2 in combination with Algorithm 2 clarifies that the total runtime of our fused approach, including any reruns, equals $((C_{\text{rerun}} - 1)T_{\text{STP}} + T_{\text{fused}}) \cdot N_{\text{fused}}$. This runtime has to be smaller than $T_{3 \text{ steps}} \cdot N_{3 \text{ steps}}$ to make the reordering of steps pays off. N_{fused} is the number of time steps required by the fused algorithm, $N_{3 \text{ steps}}$ is the number of time steps required by the baseline. To make the fusion pay off, the total time of the fused scheme has to be smaller or equal to a straightforward implementation. We obtain

$$1 \leq C_{\text{rerun}} < 1 + \frac{N_{3 \text{ steps}} \cdot T_{3 \text{ steps}} - N_{\text{fused}} \cdot T_{\text{fused}}}{N_{\text{fused}} \cdot T_{\text{STP}}},$$

with a trivial lower bound. We insert $N_{\text{fused}} = \frac{1}{C_{\Delta T}} N_{3 \text{ steps}}$.

Corollary 4 clarifies that there exists a trade-off between the cost of the STP reruns and the time step size damping: The smaller we make $C_{\Delta T}$, the smaller C_{rerun} but the larger N_{fused} . Balancing can be delicate.

Our gliding average in Alg. 2 induces $N_{\text{fused}} \geq \frac{1}{C_{\Delta T}} N_{3 \text{ steps}}$, i.e. we damp the effective ΔT further. This inequality seems to harm the corollary's upper bound. Yet, as long as the admissible time step size increases slowly or remains invariant, the inequation holds trivially. No reruns occur. Occasional reductions of ΔT_{adm} to no more $C_{\Delta T}$ of the previous admissible time step size do not lead to reruns and thus make the inequality hold more robustly. The corollary quantifies how often the admissible time step size may decrease more dramatically.

Corollary 5 *We assume that any individual tasks can complete in cache. We furthermore assume that data is completely removed from the cache if it is not reused a small, fixed number of algorithmic steps later by another task. The weak single-touch theorem alters the number of data reads and writes per time step by the ratio*

$$0.875 \leq \frac{(4d+2)C_{\text{rerun}} + 12d + 1}{18d + 4} \leq 1.125.$$

Proof 3 *The STP reads in the old time step, and determines all data along the cell's hull (Corollary 3). The Riemann solver reads in $Q_h^{*\pm}$ and $F(Q_h^{*\pm}) \cdot n$ and writes out F_h^* into both $F(Q_h^{*\pm}) \cdot n$ arrays. Neglecting the domain boundary, there are d faces per cell. The Corrector reads in the face data—the `integrateVolume` already has been anticipated by the STP—and performs the remaining tasks. We have*

$$\underbrace{8dm(p+1)^d}_{\text{Riemann reads}} + \underbrace{4dm(p+1)^d}_{\text{Riemann writes}} + \underbrace{2dm(p+1)^d + m(p+1)^d}_{\text{Corrector reads}} + \underbrace{m(p+1)^d}_{\text{Corrector writes}} + \underbrace{m(p+1)^d}_{\text{STP reads}} + \underbrace{4dm(p+1)^d + m(p+1)^d}_{\text{STP writes}}.$$

Our fused scheme kicks off a grid traversal with the *Riemann* reads. We assume that a cache-oblivious or cache-aware traversal order is chosen [4]. In our case, we exploit the Peano space-filling curve [1]. *Riemann* writes thus remain in cache for the subsequent correction. Hence, the *Corrector* solely has to read in the Q_h^* values stored in the D_h data structure to determine the next solution (written to memory). This output is handed over to the next *Predictor* immediately, i.e. the *Predictor* works in cache and does not have to reload data. It writes out the cell's space-time hull. If the optimistic time stepping runs into a rerun, we have to reload the old time step and perform the prediction again:

$$\underbrace{8dm(p+1)^d}_{\text{Riemann reads}} + \underbrace{4dm(p+1)^d}_{\text{Riemann writes}} + \underbrace{m(p+1)^d}_{\text{Corrector reads}} + \underbrace{m(p+1)^d}_{\text{Corrector writes}} + \underbrace{4dm(p+1)^d + m(p+1)^d}_{\text{STP writes}} + (C_{\text{rerun}} - 1) \cdot \left(\underbrace{m(p+1)^d}_{\text{STP reads}} + \underbrace{4dm(p+1)^d + m(p+1)^d}_{\text{STP writes}} \right).$$

The memory pressure of fused time stepping compared to a straightforward version reduces if C_{rerun} remains reasonably small: we transfer data less frequently. Our approach falls into the second rubric of communication-avoiding techniques, and, from a memory point of view, also fits rubric five. Both estimates are too pessimistic for global time stepping. Here, it is convenient to run `integrateFace` directly after the actual Riemann solver. Explicit spanning (and storing) the Riemann solution F_h^* over the time span is not required.

Corollary 6 *Our fused and shifted approach homogenises the concurrency level and reduces memory access bursts. Yet, it reduces the overall concurrency level slightly.*

We assume that we traverse the grid \mathbb{T} with multiple threads. With multithreading, we have to ensure that no two faces in Algorithm 2 are subject to the Riemann solver concurrently or “solved” twice.

Proof 4 *Running ADER-DG’s three steps one after another means that we run into step STP with concurrency level $|\mathbb{T}|$ and very high arithmetic intensity, then perform the Riemann solves with concurrency $|d \cdot \mathbb{T}|$, and finally run again a step with level $|\mathbb{T}|$. $\frac{T_{\text{STP}}}{T_{3 \text{ steps}}}$ quantifies the fraction of the runtime spent in the predictor. For a straightforward implementation, we thus obtain a time-averaged concurrency level of*

$$CL_{\text{avg}} \approx \frac{T_{\text{STP}}}{T_{3 \text{ steps}}} \cdot |\mathbb{T}| + \left(1 - \frac{T_{\text{STP}}}{T_{3 \text{ steps}}}\right) d \cdot |\mathbb{T}| = \left(d + (1 - d) \frac{T_{\text{STP}}}{T_{3 \text{ steps}}}\right) |\mathbb{T}|.$$

Our shifted and fused variant exhibits an overall homogeneous concurrency level of roughly $|\mathbb{T}|$: We merge all three algorithmic steps, i.e. process all the cells in parallel. Per cell, we have to ensure all faces have been subject to the Riemann solve first. This induces only a brief startup cost however, since arithmetically heavy `predict` tasks are overlapped with the Riemann solves. $CL_{\text{avg}} \geq |\mathbb{T}|$.

Our approach falls into the third rubric of communication-avoiding techniques as bursts of data reads or writes over the bus are avoided. We note that the difference in concurrency levels disappears for increasing STP cost and that a high concurrency level for low-cost tasks does not automatically induce high speedups.

Corollary 7 *In a non-overlapping domain decomposition, we can hide data exchange behind the traversal.*

The distributed-memory parallelisation of ADER-DG with message passing is conceptionally simple. We rely on a non-overlapping domain decomposition where the Riemann problems along the parallel subdomain boundaries are solved redundantly. Each rank sends out its projected Q_h^* and $F(Q_h^*) \cdot n$ values to the neighbouring ranks once the `extrapolate` task has terminated. All other operations are rank-local.

Proof 5 *We restrict to a machine model where the ADER-DG steps are synchronised and reiterate that `predict` is the arithmetically most demanding task. It implies that messages holding extrapolated data have, in a straightforward implementation, up to $\min(T_{\text{STP}}, T_{\text{fused}} - T_{\text{STP}})$ time to arrive at their destination rank, if we choose the task ordering optimally and manage to exchange all data non-blocking. The first message sent out has a maximal arrival time (slack) of T_{STP} . The last predicted value will the latest be required by the last Riemann solve. The time span in-between is bounded by $T_{\text{fused}} - T_{\text{STP}}$.*

For our fused and shifted algorithm, we may assume that the slack given to a message to run through the system is bounded by T_{fused} if we choose a proper task ordering on each rank. The statement holds as

$$T_{\text{STP}} \leq T_{\text{fused}} \Rightarrow \min(T_{\text{STP}}, T_{\text{fused}} - T_{\text{STP}}) \leq T_{\text{fused}}.$$

We could harm the right condition iff $T_{\text{STP}} > \frac{1}{2}T_{\text{fused}}$ and $T_{\text{fused}} - T_{\text{STP}} > T_{\text{fused}}$. However, $T_{\text{fused}} - T_{\text{STP}} > \frac{1}{2}T_{\text{fused}} > T_{\text{fused}}$ cannot hold.

Our approach falls into the fourth rubric of communication-avoiding algorithms, as we reduce the criticalness of data communication. Rubric five applies automatically. Localisation of data transfer (rubric five) is implicitly given by ADER-DG—as for any explicit scheme—as information almost exclusively is transferred through the faces.

7 Results

We conducted our experiments on an Intel E5-2650V4 (Broadwell) cluster with 24 cores per node. They run at 2.4 GHz and are connected by Omnipath. All hardware counters have been evaluated through Likwid [20]. Furthermore, we ran our experiments on KNL processors (Xeon Phi 7210) with 64 cores each. They run at 1.30 GHz. For the shared memory parallelisation, we rely on Intel’s Threading Building Blocks (TBB) while Intel MPI is used for the distributed memory parallelisation. Intel’s 2017 C++ compiler translated all codes.

Table 2: Performance counters tracking the memory bus usage for a $27 \times 27 \times 27$ grid on one node. Smooth initial conditions ensure that $C_{\text{rerun}} = 1$. The upper part holds data from the straightforward implementation with three distinct steps, i.e. $T = T_{3 \text{ steps}}$. The lower part holds data from our fused approach ($T = T_{\text{fused}}$). Both approaches follow Corollary 3. The bandwidth (BW) is given as MB/s, the volume (Vol.) transferred is given in GB. All timings are time per time step with $[T] = s$.

p	1 core			12 cores			24 cores		
	BW	Vol.	T	BW	Vol.	T	BW	Vol.	T
3	1,357.44	30.59	1.36	2,885.94	35.24	0.75	4,639.00	73.32	0.71
5	1,155.42	101.64	3.91	4,158.00	117.06	1.25	6,377.94	223.06	1.04
7	806.87	215.91	14.75	5,695.60	285.40	2.24	8,540.10	520.33	1.83
9	483.04	487.98	29.20	20,894.15	4,376.39	4.66	30,938.36	4,716.02	3.76
3	1,233.97	24.05	1.14	3,645.78	31.58	0.39	5,481.20	71.92	0.39
5	861.10	80.49	4.18	5,931.70	110.40	0.68	8,403.62	211.44	0.57
7	625.40	176.84	10.71	6,877.66	350.95	1.98	9,003.53	621.64	1.50
9	429.35	434.20	25.96	17,525.00	4,619.24	4.80	27,297.87	5,280.57	4.32

Our runtime analysis focuses on compressible Euler equations with $m = 5$, $B = S = 0$ and no δ impact in (1). We study

$$\frac{\partial}{\partial t} Q + \nabla \cdot F(Q) = 0 \text{ with } Q = \begin{pmatrix} \rho \\ j \\ E \end{pmatrix}, F = \begin{pmatrix} j \\ \frac{1}{\rho} j \otimes j + pI \\ \frac{1}{\rho} j (E + p) \end{pmatrix}, p = 0.4 \left(E - \frac{1}{2\rho} (j, j) \right).$$

$\rho, E : \Omega \mapsto \mathbb{R}$ encode the scalar density and the energy, while the vector $j : \Omega \mapsto \mathbb{R}^d$ holds the medium’s velocities. A pressure p calibrates the whole setup. \otimes is the outer dot product.

For communication-avoiding algorithms, this is a challenging setup as the PDE is simple. Its arithmetic intensity per ADER-DG step is low compared to more complicated PDEs such as seismic or gravitational waves. No implementational and communication flaws are hidden by computations.

7.1 Hardware counter

We start our experiments with studies of the hardware counters on a single core (Table 2). A straightforward implementation with three grid sweeps per ADER-DG time step acts as baseline. It already stores solely the space-time cell hull. Fusion of all ADER-DG steps into a single-touch code reduces the data running through the memory bus to 0.79–0.89 of the baseline. This reduction translates into diminished bandwidth requirements. Besides one outlier for $p = 5$ where the bandwidth drops dramatically—we are not able to identify the reason for this—the application of our techniques speeds up the code.

If we use one socket or all cores of the node, our optimisations increase the amount of doubles transferred over the bus once $p \geq 7$. Parallel to this, the used bandwidth now increases. Besides for $p = 9$, fusion rather robustly speeds up the code; the poor scalability is a strong scaling effect and scalability overall is subject of study next. In all of our experiments, the L2 cache miss rate of the optimised code variant is in the order of 2% with occasional outliers up to 4.92%. The L3 miss rate is 0.1% at most. While cache misses basically do not exist, we see a rapid increase in the L3 access bandwidth for the multicore experiments once we increase p beyond 5. With Stream TRIAD [15] yielding around 17,774.3 MB/s on a single core and 121,495.2 MB/s on all 24 cores, our code is not bandwidth-bound. Besides for $p = 3$, our optimisation techniques increase the MFLOPS/s by a factor of 1.7–2. The growth in MFLOPS/s scales with p .

Corollary 5 predicts for $C_{\text{rerun}} = 1$ and $d = 3$ a reduction of the memory transfer demands to 0.775. This matches our single core observations. In general, the corollary predicts a reduction of the memory volume for $C_{\text{rerun}} < 1.5$ as long as we assume that the idea behind Corollary 3 has been applied. If we made the comparison’s baseline, i.e. the three step

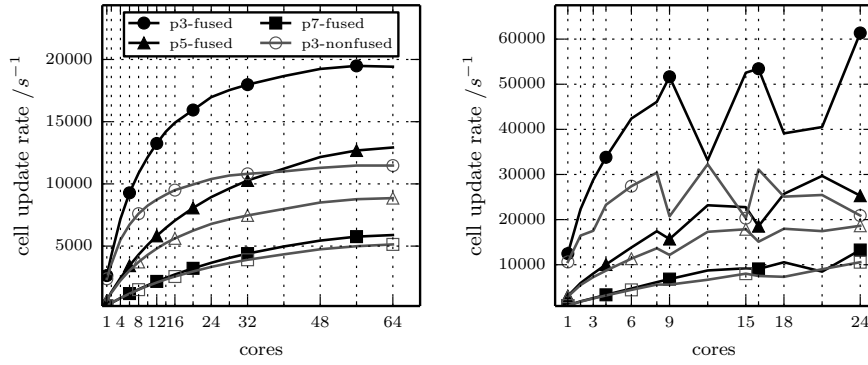


Figure 2: Characteristic shared memory profiles for $d = 3$ on KNL (left) and Broadwell (right).

implementation, hold the complete space-time polynomials and fluxes too, the single-touch reordering reduced the transferred data for all $C_{\text{rerun}} \leq 2.0$.

The caveat in practice is Corollary 4. For the present setups and a $C_{\Delta T} = 0.99$, we experimentally obtain maximum values of C_{rerun} between 1.21 ($p = 3$) down to 1.01 ($p = 7$) and 0.98 ($p = 9$) on a single core. These values demonstrate that reruns have to be avoided the more rigorously the higher the cost of the predictor. Yet, naively reducing the safety value $C_{\Delta T}$ does not work either. If $C_{\Delta T}$ is chosen too pessimistic, i.e. too small, the fusion even might not pay off at all. The optimistic time stepping requires too many additional steps through the safety factor (cmp. data for $p = 9$). To make our approach perform, a user has to balance $C_{\Delta T}$ and ensure that the number of reruns remains below a problem- and machine-specific threshold. Fortunately, this upper threshold on C_{rerun} increases if we increase the core count as T_{STP} is almost embarrassingly scaling.

The merging and reordering of the algorithmic steps in combination with an SFC-based grid traversal which is spatially and temporally localised [22] plus the storage of solely the space-time hull yields a cache-oblivious code. The MFLOPS/s increase due to the fusion of steps and the optimistic time stepping. Though our techniques are designed to optimise the memory access, they allow the compiler to exploit the vector facilities better; even for our PDE with low arithmetic intensity. They team up with the common knowledge that we have to increase the polynomial order to increase the arithmetic intensity.

The optimisations’ homogenisation of the concurrency level and the storage of solely the cell hull are a double-edged sword. STP temporarily has to hold all space-time unknowns per cell. If the code runs in parallel, each thread has to allocate these temporary data. The memory demands scale with both p and the core count. Though the code exhibits advantageous cache access characteristics, some data now is evacuated from the high-level and last-level caches and then brought in again. For $p = 9$, solely T_{STP} dominates the runtime. Fusing tasks and thus intermixing and nonhomogenising memory accesses here makes the code become inferior to a non-fused approach where STP streams data with quasi-uniform operations through the cores. With increasing last level cache sizes as they come along with an KNL, e.g., this performance “anomaly” will disappear.

7.2 Shared memory scalability

We continue with scalability tests on single nodes (Fig. 2) where we apply sufficiently smooth initial conditions plus a $C_{\Delta T}$ to ensure that $C_{\text{rerun}} = 1$. We omit rerun effects. Our techniques yield, for most of the setups, better runtimes than their straightforward counterpart using three grid sweeps for the three algorithmic steps. On the multicore chip, the data are ragged while the manycore yields smooth curves. Both curves show a widening speed gap, i.e. the more cores we use the more important our optimisations. Yet, the higher the polynomial degree p , the less important our optimisations.

A straightforward implementation exhibits three synchronisation points per realisation

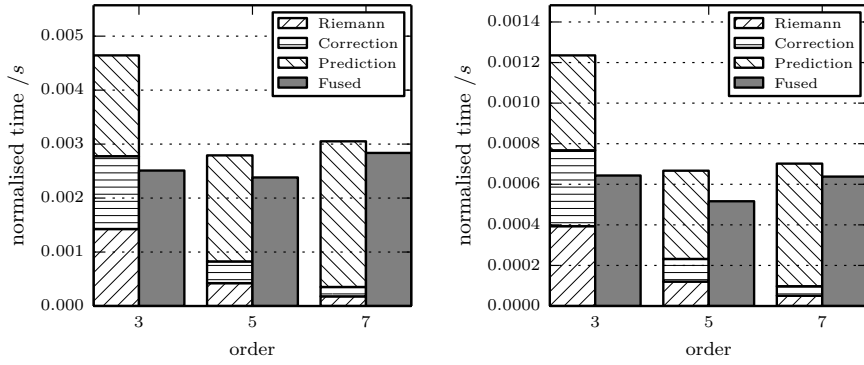


Figure 3: Time per time step for a $81 \times 81 \times 81$ mesh on KNL (left) and Broadwell (right). 28 ranks are used. The time is normalised w.r.t. the $81^3 \cdot (p + 1)^3$ Legendre points of the solution.

time step with two of the phases in-between (**Riemann** and **Corrector**) being cheap. Relative to STP, they become almost serial tiny phases for growing polynomial order. Amdahl’s law clarifies that the two cheap phases tend to throttle the upscaling. Our techniques eliminate two out of three synchronisation points per realisation time step. This way, they make the code scale better. The gap between the two implementation variants widens. Yet, the scaling improvement is constrained by the reduced concurrency level from Corollary 6. The closer T_{STP} to $T_{3 \text{ steps}}$, i.e. the higher p , the harsher the reduction of the concurrency level. The relative gain in performance through the optimisation techniques reduces with growing polynomial degree.

On both architectures, our techniques pay off most for the smaller p choices—in particular for Finite Volumes—for tiny time step sizes where few Picard iterations are required, and for linear variants of (1) where the cost ill-balance between STP and other phases is not too significant.

7.3 Distributed memory characteristics

We close the experiments with distributed memory tests realised through MPI. Shared memory parallelisation is disabled to avoid that different runtime effects interfere. All experiments are chosen such that the analysis covers only simulation spans where the work is reasonably good balanced. No ill-balancing pollutes the data. Finally, the setup is chosen such that no reruns are observed. Fused time stepping continues to pay off throughout all of our experiments (cmp. exemplary Fig. 3). The pay off however is limited on the manycore. Effectively, the measured time for the fused approach equals the time required for the sole STP grid sweep. Given the massive growth of STP cost for increasing polynomial degrees, fusion’s impact is more significant for small p .

ADER-DG’s prediction triggers data exchange through the cell faces. This data has to arrive for the subsequent Riemann solves whereas no data transfer is required when we progress from the Riemann solutions to the correction step. All results suggest that all the data exchange is successfully hidden behind the computation. The predictor dominates the parallel runtime, but almost all data exchange happens in the background of this STP as we do not see a significant increase of the **Riemann** timings. The improvement characteristics of our fused, communication-avoiding ADER-DG variant are preserved for distributed memory runs.

Two insights put this success into perspective: The hiding of communication applies for the non-fused realisation, too. It is solely the immediate firing of Riemann input data by the STP tasks that makes the data transfers hiding behind computations. The other techniques have no positive impact. Instead, only lower p orders yield $T_{fused} + T_{STP} < T_{3 \text{ steps}}$. The optimistic time stepping remains not without risk for parallel runs, i.e. have to be avoided for higher polynomial order.

8 Conclusion

Our manuscript details the implementation of an ADER-DG code that exhibits communication-avoiding characteristics. For this, we generalise and detailed the term communication-avoiding itself. Our experimental data with ADER-DG employing a Finite Volume limiter plus our analyses suggest that the techniques pay off. The techniques or variations of them apply and are of use for a vast range of predictor-corrector schemes in general.

There are two natural extensions of the present research. They are subject to ongoing work. On the one hand, we have to demonstrate the impact and usefulness of the presented techniques for real-world simulation challenges. This is part of the ExaHyPE [2] agenda. On the other hand, we have to detail how grid layouts and implicitly generated task graphs as well as grid traversals and implicitly defined task graph processing interplay. This is important for real-world scaling. Our results suggest that tasks aligning along subdomain boundaries in an MPI context are critical, i.e. have to be handled as soon as possible. Prioritised processing allows the corresponding Riemann input data to squeeze through the network while further tasks are processed. Also, we do present MPI results for given setups which illustrate the effectiveness of the proposed solutions. Appropriate load balancing has been enforced manually. In practice, the quality of the load balancing in context with the tasking will determine the achieved performance.

Acknowledgements

The authors appreciate support received from the European Unions Horizon 2020 research and innovation programme under grant agreement No 671698 (ExaHyPE). This work made use of the facilities of the Hamilton HPC Service of Durham University, and it used the ARCHER UK National Supercomputing Service (<http://www.archer.ac.uk>), i.e. its KNL nodes. Thanks are due to all members of the ExaHyPE consortium who made this research possible. Particular assistance with the numerical scheme has been provided by Michael Dumbser. All underlying software is open source [2].

References

- [1] M. BADER, *Space-Filling Curves*, vol. 9 of Texts in Computational Science and Engineering, Springer Berlin Heidelberg, Berlin, Heidelberg, 2013.
- [2] M. BADER, M. DUMBSER, A. GABRIEL, H. IGEL, L. REZZOLLA, AND T. WEINZIERL, *ExaHyPE—an Exascale Hyperbolic PDE solver Engine*, 2017.
- [3] G. BALLARD, D. BECKER, ET AL., *Communication-avoiding symmetric-indefinite factorization*, SIAM J. Matrix Analysis Applications, 35 (2014), pp. 1364–1406.
- [4] H.-J. BUNGARTZ, M. MEHL, T. NECKEL, AND T. WEINZIERL, *The PDE framework Peano applied to fluid dynamics: an efficient implementation of a parallel multiscale fluid dynamics solver on octree-like adaptive Cartesian grids*, Computational Mechanics, 46 (2010), pp. 103–114.
- [5] J. DEMMEL, *Communication avoiding algorithms*, in 2012 SC Companion: High Performance Computing, Networking Storage and Analysis, 2012, pp. 1942–2000. (presentation).
- [6] J. DONGARRA, J. HITTINGER, ET AL., *Applied Mathematics Research for Exascale Computing*, 2014. DOE ASCR Exascale Mathematics Working Group: <http://www.netlib.org/utk/people/JackDongarra/PAPERS/doe-exascale-math-report.pdf>.
- [7] M. DUMBSER AND M. KÄSER, *An arbitrary high-order discontinuous Galerkin method for elastic waves on unstructured meshes - II. The three-dimensional isotropic case*, Geophysical Journal International, 167 (2006), pp. 319–336.

- [8] M. DUMBSER, O. ZANOTTI, R. LOUBRE, AND S. DIOT, *A posteriori subcell limiting of the discontinuous Galerkin finite element method for hyperbolic conservation laws*, Journal of Computational Physics, 278 (2014), pp. 47–75.
- [9] W. ECKHARDT, R. GLAS, D. KORZH, S. WALLNER, AND T. WEINZIERL, *On-the-fly memory compression for multibody algorithms*, in Advances in Parallel Computing 27: International Conference on Parallel Computing (ParCo) 2015, G. Joubert, H. Leather, M. Parsons, F. Peters, and M. Sawyer, eds., vol. 27, IOS Press, 2016, pp. 421–430.
- [10] G. GASSNER, M. DUMBSER, F. HINDENLANG, AND C.-D. MUNZ, *Explicit one-step time discretizations for discontinuous Galerkin and finite volume schemes based on local predictors*, Journal of Computational Physics, 230 (2011), pp. 4232–4247.
- [11] P. GHYSELS, T. ASHBY, K. MEERBERGEN, AND W. VANROOSE, *Hiding global communication latency in the gmres algorithm on massively parallel machines*, SIAM Journal on Scientific Computing, 35 (2013), pp. C48–C71.
- [12] J. HESTHAVEN AND T. WARBURTON, *Nodal discontinuous Galerkin methods: algorithms, analysis, and applications*, no. 54 in Texts in applied mathematics, Springer, 2008.
- [13] M. JABBAR, G. MARKOMANOLIS, H. IBEID, R. YOKOTA, AND D. KEYES, *Communication reducing algorithms for distributed hierarchical n-body problems with boundary distributions*, in High Performance Computing - 32nd International Conference, ISC High Performance 2017, Frankfurt, Germany, June 18-22, 2017, Proceedings, J. Kunkel, R. Yokota, P. Balaji, and D. Keyes, eds., vol. 10266 of Lecture Notes in Computer Science, 2017, pp. 79–96.
- [14] M. KOWARSCHIK AND C. WEI, *An overview of cache optimization techniques and cache-aware numerical algorithms*, in Algorithms for Memory Hierarchies Advanced Lectures, volume 2625 of Lecture Notes in Computer Science, Springer, 2003, pp. 213–232.
- [15] J. MCCALPIN, *Memory bandwidth and machine balance in current high performance computers*, IEEE Computer Society Technical Committee on Computer Architecture (TCCA) Newsletter, (1995), pp. 19–25.
- [16] J. REINDERS, *Intel Threading Building Blocks*, O’Reilly, 2007.
- [17] B. REPS AND T. WEINZIERL, *A complex additive geometric multigrid solver for the helmholtz equations on spacetrees*, ACM Transactions on Mathematical Software, (2016). accepted.
- [18] H. SUNDAR, R. S. SAMPATH, AND G. BIROS, *Bottom-up construction and 2:1 balance refinement of linear octrees in parallel*, SIAM Journal on Scientific Computing, 30 (2008), pp. 2675–2708.
- [19] V. A. TITAREV AND E. F. TORO, *ADER: Arbitrary high order Godunov approach*, Journal of Scientific Computing, 17 (2002), pp. 609–618.
- [20] J. TREIBIG, G. HAGER, AND G. WELLEIN, *LIKWID: A Lightweight Performance-Oriented Tool Suite for x86 Multicore Environments*, in Proceedings of the 2010 39th International Conference on Parallel Processing Workshops, ICPPW ’10, IEEE Computer Society, 2010, pp. 207–216.
- [21] M. WEINZIERL AND T. WEINZIERL, *Quasi-matrix-free hybrid multigrid on dynamically adaptive cartesian grids*, ACM Transactions on Mathematical Software, pp. 2732–2760. (submitted; arXiv:1607.00648).
- [22] T. WEINZIERL, *The Peano software—parallel, automaton-based, dynamically adaptive grid traversals*, ACM Transactions on Mathematical Software, (2017). (submitted; arXiv:1506.04496).

- [23] T. WEINZIERL AND M. MEHL, *Peano—A Traversal and Storage Scheme for Octree-Like Adaptive Cartesian Multiscale Grids*, SIAM J. Sci. Comput., 33 (2011), pp. 2732–2760.
- [24] A. YARKHAN, J. KURZAK, P. LUSZCZEK, AND J. DONGARRA, *Porting the plasma numerical library to the openmp standard*, International Journal of Parallel Programming, 45 (2017), pp. 612–633.
- [25] O. ZANOTTI, F. FAMBRI, M. DUMBSER, AND A. HIDALGO, *Spacetime adaptive ADER discontinuous Galerkin finite element schemes with a posteriori sub-cell finite volume limiting*, Computers & Fluids, 118 (2015), pp. 204 – 224.

A Finite Volume schemes within the predictor-corrector formalism

Corollary 8 *Finite Volumes with Rusanov fluxes can be cast into a predictor-corrector scheme.*

Proof 6 *Let $p = 0$ and let the predictor be the identity, i.e. the predicted solution $Q_h^*(T + \Delta T) = Q_h(T)$: We make `extrapolate` write Q_h^* and a $F(Q_h^*)$ onto the 2d faces of each cell and write `idc→∂c`. With this information, `Riemann` determines $\frac{1}{2}(Q_h^+ + Q_h^-) + \alpha \cdot (F_h^+ - F_h^-)$. We write `solveRiemann=computeRusanovFluxes`. As $p = 0$, both integration tasks multiply their input with ΔT , i.e. (6) becomes*

$$Q_h(T + \Delta T) = (id + \Delta T \cdot \text{computeRusanovFluxes} \circ id_{c \rightarrow \partial c}) Q_h(T).$$

The result is not surprising as we constructed our ADER-DG data structures to support (space-time) Rusanov solvers. Yet, the corollary illustrates how the limiter is to be realised: Here we embed $(2d + 1)^d$ patches into each ADER-DG cell. The subdivision, i.e. the patches, compensate for the high order. As patches are equivalent to $p = 0$ ADER-DG on a subgrid, the faces of our limiter hold $(2p + 1)^{d-1}$ Q/F -tupels as opposed to $(2p + 1)^d$ space-time entries. The Finite Volume scheme has lower total memory demands, but otherwise allows for exactly the same data flow and algorithmic step paradigms.

Corollary 9 *Finite Volumes with a MUSCL-Hancock Riemann solvers can be cast into our ADER-DG predictor-corrector formalism if we (i) restrict to tensor-product style operators, i.e. neglect interaction of a Finite Volume cell with neighbours that are not face-connected, and (ii) rely on patches of at least two Finite Volume cells per coordinate axis per cell.*

Proof 7 *We preserve the constant extrapolation in time in the predictor from Corollary 8. While we project $Q_h^* = Q_h$ onto the face, we do not map the corresponding flux onto the face as we observe that $Q_h^* = Q_h$ implies that these fluxes hold redundant information anyway. Instead we project the gradients (weighted difference) of $Q_h(T)$ to the faces.*

With the second entry on the face, i.e. the F entry, holding $(\nabla Q_h^, n)^-$ and $(\nabla Q_h^*, n)^+$, we can reconstruct the Q values of neighbour of neighbour cells along a coordinate axis. Indeed, it is reasonable to technically store those values directly in F instead of gradients along a normal. Knowing neighbours of neighbours allows us to realise MUSCL-Hancock’s internal prediction for half time steps with the `Riemann` task. The overall scheme follows the proof of Corollary 8 with `solveRiemann=computeMUSCLHancockFlux`.*

B Proof of Corollary 2

Proof 8 *ADER-DG’s minimalist version (without limiter and adaptive mesh refinement, e.g.) runs three steps per time step which decompose into individual tasks. `STP` and `Corrector` are defined on one cell, while `Riemann` accepts input data from two cells. Explicit time stepping means that ADER-DG runs a sequence of steps `STP` $\sqsubseteq_{\text{before}}$ `Riemann` $\sqsubseteq_{\text{before}}$ `Corrector` $\sqsubseteq_{\text{before}}$ `STP` $\sqsubseteq_{\text{before}}$ `Riemann` $\sqsubseteq_{\text{before}}$ \dots . Element-wise single-touch means that there is a splitting of this sequence into chunks of three tasks such that the data Q_h of any cell is read and written only once per task triad. We assume that such a splitting exists. The periodicity of the sequence implies that we have to analyse three variants to find it.*

We first assume that we can split up ADER-DG into $(STP \sqsubseteq_{\text{before}} \text{Riemann} \sqsubseteq_{\text{before}} \text{Corrector})^+$ step sequences. Let c_a be subject to *STP*. We have to assume that it yields the input to *Riemann* for one face while the data from the face-connected neighbouring cell c_b is already available. Consequently $c_b \sqsubseteq_{\text{before}} c_a$. To ensure a single touch, *Corrector* on c_a follows immediately to the *Riemann* solve. This means the code is not single-touch for c_b .

We second assume that we can split up ADER-DG into $STP \sqsubseteq_{\text{before}} (\text{Riemann} \sqsubseteq_{\text{before}} \text{Corrector} \sqsubseteq_{\text{before}} STP)^+$ step sequences. The single touch constraint here is rewritten from a cell-based notion into a face-based notion, i.e. face information is used to keep multiple time steps consistent. To ensure single touch, we have for any cell c_a to run *STP* directly after *Corrector*. *Corrector* comprises a task `calcTimeStepSize` (Table 1). Without further assumptions on the time stepping scheme, i.e. that the solution evolves smoothly and ΔT_{adm} thus is continuously increasing, a cell c_b with $STP(c_a) \sqsubseteq_{\text{before}} STP(c_b)$ might reduce the admissible time step used for c_a . We thus have to recompute $STP(c_a)$ and are not single touch anymore.

We finally assume that we can split up ADER-DG into $STP \sqsubseteq_{\text{before}} \text{Riemann} \sqsubseteq_{\text{before}} (\text{Corrector} \sqsubseteq_{\text{before}} STP \sqsubseteq_{\text{before}} \text{Riemann})^+$ step sequences. While this is indeed single-touch w.r.t. cell data, the previous argument on the exchange of admissible time step sizes ΔT_{adm} continues to hold.

Our assumption that there is a single-touch element-wise algorithm has been wrong.

C Technical details on the properties

Proof for Corollary 3 A straightforward implementation of ADER-DG exhibits at least the following persistent memory footprint per cell following Table 1. *STP* works on the following data cardinalities:

$$\underbrace{m(p+1)^d}_{Q_h} + \underbrace{(d+1)m(p+1)^{d+1}}_{\text{from predict}} + \underbrace{4dm(p+1)^d}_{\text{from extrapolate}}$$

The *Riemann* solve yields F_h^* over space-time though space here refers to cell faces only. The result is to be stored in a separate data structure. Again, all quantities are normalised w.r.t. cell count:

$$\underbrace{2dm(p+1)^d}_{\text{from solveRiemann}}$$

The actual update can be performed in-situ in Q_h . Time step size computations do not increase the memory footprint which totals in

$$(d+1)m(p+1)^{d+1} + (1+6d)m(p+1)^d.$$

The present paper's variant induces, according to Table 1, a memory footprint of

$$\underbrace{2m(p+1)^d}_{Q_h \text{ and } D_h} + \underbrace{4dm(p+1)^d}_{\text{from extrapolate}} + \underbrace{2dm(p+1)^d}_{\text{from solveRiemann}} = (2+6d)m(p+1)^d.$$

We obtain a relative memory footprint of our implementation compared to a straightforward, 3-step code of

p	$d = 2$	$d = 3$
2	0.64	0.65
3	0.56	0.57
4	0.50	0.51
5	0.45	0.47
6	0.41	0.43
7	0.38	0.39
8	0.35	0.36
9	0.33	0.34

Remarks on Corollary 6 The concurrency models in Corollary 6 lack the fact that all three phases (in the straightforward variant) or the fused approach, respectively, contain tiny serial fragments plus startup cost. These fragments materialise in limited scalability in our results.

The inequality itself follows trivially from

$$d + (1 - d) \frac{T_{\text{STP}}}{T_{3 \text{ steps}}} \Rightarrow 2 - \frac{T_{\text{STP}}}{T_{3 \text{ steps}}} \geq 1 \quad \text{for } d = 2,$$

$$3 - 2 \frac{T_{\text{STP}}}{T_{3 \text{ steps}}} \geq 1 \quad \text{for } d = 3$$